

WEAR PROPERTIES OF SURFACE ALLOYED STEEL WITH TUNGSTEN AND BORON BY TIG WELDING

ABAKAY Eray, DURMAZ Mustafa, SEN Saduman, SEN Ugur

¹*Sakarya University, Engineering Faculty, Metallurgical & Materials Engineering Department, Esentepe Campus, Sakarya, Turkey*

eabakay@sakarya.edu.tr, mdurmaz@sakarya.edu.tr, sdmnsen@sakarya.edu.tr, ugursen@sakarya.edu.tr

Abstract

In this study, effect of boron addition to Fe-W hardfacing alloys was investigated. The Fe-W and the Fe-W-B based hardfacing alloys were deposited on AISI 1020 steel substrates by a manual tungsten-inert-gas (TIG) hardfacing method. Obtained coatings were characterized by microstructural examinations, phase analysis and sliding wear tests. According to microstructural examinations, hardfaced samples are included three different layers which are coated zone, steel substrate and transition zone which between the coating zone and the substrate. The coating zone for the both samples cannot be shown any defect like crack or porosity. Addition of boron to the Fe-W alloy, further the Fe-W hypereutectic structure boride phases like FeWB, Fe₂W₂B and Fe₂W₂C phases formed in the coating layer. The wear tests of the samples against alumina ball were carried out by using a ball-on-disc tribometer. The friction coefficient of the alloys is changing between 0.51-0.58 depending on the loads. The main wear mechanism of the layers were oxidative, adhesive and fatigue wear.

Keywords: Hardfacing alloys, sliding wear, microstructure, borides

1. INTRODUCTION

As for engineering machines and components, there is an ever-increasing demand for the wear resistant materials, which can reduce wear and thus extend their service life. Such composite hardfacing coatings, commonly known as in-situ composites. Especially, hyper-eutectic in-situ composites included boron can significantly improve the tribological properties of components by employing a metallic alloy as the matrix and the boron based ceramic massive phases beside eutectic microstructure of the boride phase and the solute solution of the based metal [1]. Among all the reinforcements, boride phases are often chosen because of their lower density and the fact that their hardness is similar to other reinforcements [2]. Tungsten borides are known to have high hardness values, chemical inertness and electronic conductivity. Four different compounds in W-B binary system are W₂B, WB, WB₂, W₂B₅ and W_{1-x}B₃ (denoted earlier as WB₄, WB₁₂ or W_{2-x}B₉). They have possible industrial applications as abrasive, corrosion-resistant and electrode materials, which are exposed to exceptional environments. Refractory borides are very hard, but also brittle. This limitation can be partially circumvented if they are used as coatings over less brittle materials like metallic alloys [3, 4].

Hardfacing technique is a kind of surface treatment to increase the wear life of erosion, abrasive and adhesive wear, damaged parts, of which hardfacing alloy that has excellent resistance to wear is deposited onto the substrate [5]. Hardfacing can be applied by several techniques, such as plasma transfer arc welding (PTAW), submerged arc welding (SAW), laser beam welding (LBW), oxyacetylene flame brazing, friction stir processing, tungsten inert gas welding (TIG), high-velocity Oxy-fuel coating (HVOF) and arc welding by electrodes [6]. The gas tungsten arc welding (TIG) process (also called GMAW welding) is used when a good weld appearance and a high quality of the weld are required. In this process, an electric arc is formed between a tungsten electrode and the base metal. The arc region is protected by a kind of inert gas or a mixture of inert gases. The tungsten electrode is heated to temperatures high enough for the emission of the necessary electrons for the operation of the arc [7]. TIG possesses the advantages of high deposition rate, high welding speed and

deep penetration. Hence, the TIG welding process is preferred over gas metal arc welding so as to obtain high quality weldments [8].

In this work, Fe-W and Fe-W-B based alloys were deposited on AISI 1020 steel substrates in order to research the effect of boron-addition on the microstructure, mechanical properties and wear behaviour of Fe-W hardfacing alloys. The main goal is to compare the wear-resistance performance of these alloys for hardfacing of the carbon steel components. As well as the effect of boron addition on the microstructure and phase formation of the hardfacing layers was investigated.

2. EXPERIMENTAL

Two different hardfacing alloys were used in this work, which are Fe-W and Fe-W-B alloys. The alloys were prepared using ball milled Armco iron, ferro-tungsten and ferro-boron powders. Selected substrates for the treatment was AISI 1020 steel, which is a low carbon and cheap material widely used in manufacturing of simple constructions and machine elements [9]. The substrates were cut to the size of 60 x 20 x 5 mm³. The chemical compositions of the substrates and the ferro-alloys were given in **Table 1**.

Table 1 The chemical compositions of the substrates and the ferro-alloys (wt. %)

Materials	C	Si	Mn	W	P	S	B	Al	Fe
AISI 1020	0.17	0.18	0.52	-	-	-	-	-	Bal.
Ferro-tungsten	0.11	0.56	0.18	77.98	0.06	0.06	-	-	Bal.
Ferro-boron	-	0.39	-	-	0.03	0.01	18.58	0.09	Bal.

TIG/GTAW welding process was used for the hardfacing treatment on the substrates manually. Before the treatment, the substrates were prepared with 60 grit emery paper and ultrasonically cleaned with acetone to remove all undesirable contaminations. After the hard-facing treatment, the samples were cooled in the air and finally subjected to microstructural, mechanical and wear examinations.

Microstructural examinations were realized by optical microscopy (Epiphot 200, Nikon, Japan) and scanning electron microscopy (JSM-6060 LV, Jeol, Japan) with energy-dispersive spectrometer (EDS). The cross-sections of the samples were ground to 1200 grid SiC emery paper, polished with 0.3 alumina suspension and etched by 2 pct Nital. X-ray diffraction (XRD) analysis was conducted by using Rigaku D-max 2200 type diffractometer with a Cu-K_α radiation, which has a wavelength of 1.54056 Å to analyze the phases present in the coatings over a 2θ range of 20-80°. A ball-on disc tribometer which made in accordance with ASTM G133-05 standard was used for the dry sliding wear tests. The tests were all conducted at room conditions with a 10 mm in diameter alumina ball as the counter-body. The sliding speed was set to 0.1 m/s and the sliding distance was approximately 250 m. The applied loads were 2.5 N, 5.0 N and 10.0 N for the tests. Mean Hertzian contact pressures calculated for alumina ball under the applied loads were 389, 491 and 618 MPa, respectively and the compressive yield strength of alumina was 2600 MPa, respectively. Wear features of the surfaces were examined using the SEM and EDS.

3. RESULTS AND DISCUSSION

Figure 1 shows the optical and SEM micrographs of the hard-faced layers. For both samples in which no cracks and porosity could be seen from the figures. From the **Figure 1 (a)** and **(b)**, it can be seen the presence of randomly dispersed Fe₇W₆ phases in W and on iron matrix, which was confirmed by XRD results, which was shown in **Figure 2 (a)**. Depending on Fe-W phase diagram, the possible phases took place in the alloyed layer are Fe₇W₆ and W-Fe solid solution of which has a needle-like morphology. As shown from the figure that the hard intermetallic phase was well distributed in the Fe-W solid solution matrix. Addition of boron in the Fe-W alloy caused to modify the structure of the alloy. As seen in **Figure 1(c)** and **(d)**, there is a eutectic

morphology included some blocky hard boride phases in. The structure of the alloyed1 layer presents the eutectic constituent structure which are formed entirely, all in and some blocky boride phases collected among the eutectic grains junctions. XRD analysis of the Fe-W-B surface alloyed layer showed that the phases formed in the layer are FeW_2B_2 , FeWB and $\text{Fe}_2\text{W}_2\text{C}$, see **Figure 2**. EDS analysis of the phases took place in the alloyed layer demonstrate that blocky phase numbered as (1) on the SEM image include Fe-W-B, and grey phase placed among the white finger print structure in the eutectic structure has Fe-W-B elements and W content is higher than that of the blocky phase. In addition, the white fingerprint structure includes Fe-W-C elements. In this case, it is possible that the blocky white phase is FeWB , the white fingerprint structure is FeW_2B_2 and grey phase took place among the white fingerprint structure is $\text{Fe}_2\text{W}_2\text{C}$ phase. **Figure 3 (a)**. There are also blocky boride phases can be seen in the structure. According to B-Fe-W ternary phase diagram, there is an accordance with the phases [10]. The results of the patterns confirm the OM and SEM images. For Fe-W alloy, the main phases are W-Fe solid solution and Fe_7W_6 . Addition of boron, FeWB and FeW_2B_2 boride phases, and $\text{Fe}_2\text{W}_2\text{C}$ phase. Transition reactive metals are strong boride and carbide forming elements and the boride phases is formed at temperatures above 700 °C in general [11 - 13].

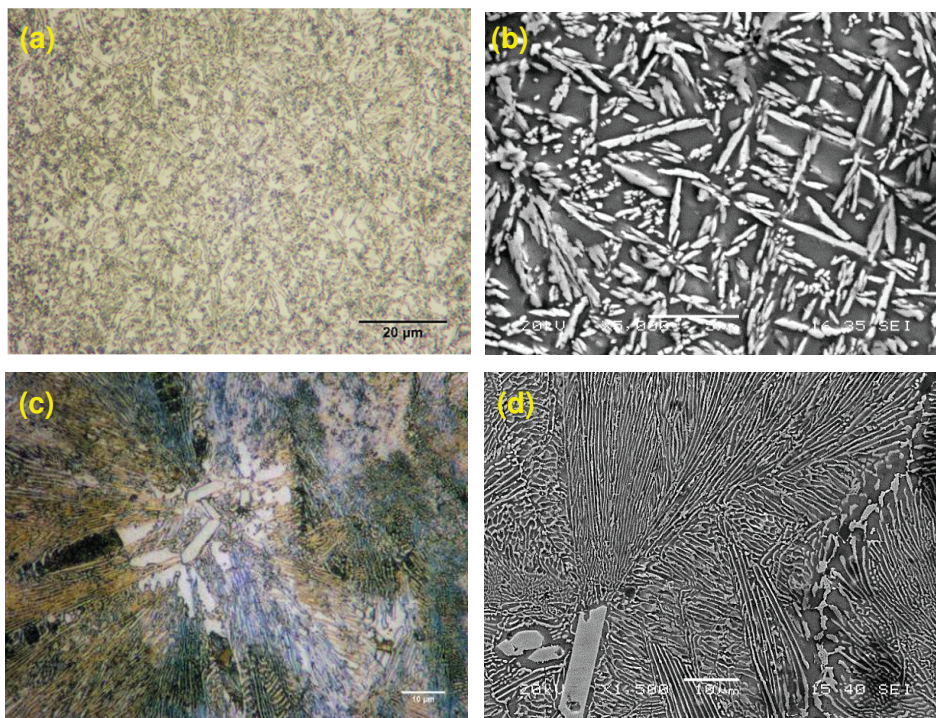


Figure 1 Optical and SEM micrographs of hardfaced AISI 1020 steel with (a-b) and (c-d) Fe-W Fe-W-B alloys, respectively

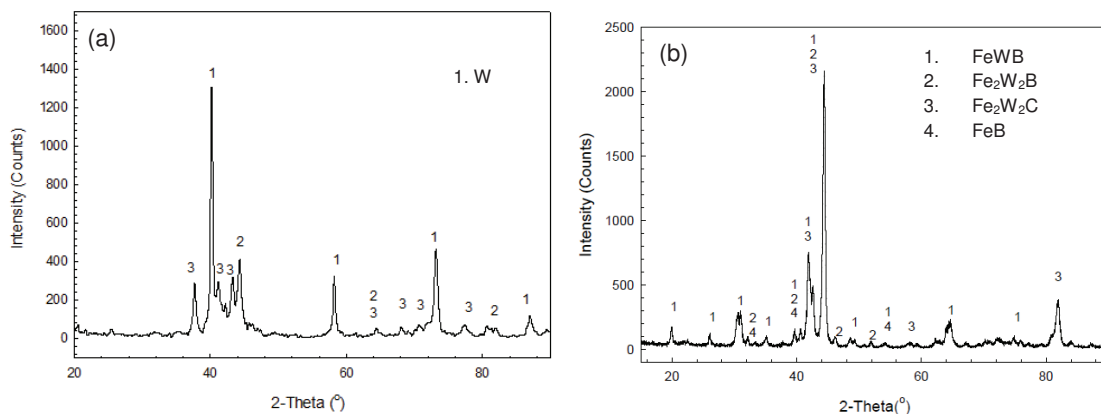


Figure 2 XRD pattern of the hardfaced with Fe-W and Fe-W-B alloy on AISI 1020 steel

Figure 3 (a) and **(b)** shows the friction coefficient curves of Fe-W and Fe-W-B hard-faced layers against alumina counterparts under the room conditions and variable loads. From **Figure 3 (a)** showed that the friction coefficient of Fe-W alloyed layer was immediately become steady-state. With an increase in load value, the friction coefficient also increased from 0.51 to 0.58. In general, friction coefficient values close up each other for applying loads, but friction coefficient values of the Fe-W surface alloyed layers depending on the applied load with sliding distance, the friction coefficient value of the layer was getting close up and increase, slightly. Friction coefficients of the Fe-W-B based surface alloyed layer were getting an increase with decreasing acceleration about 30 m and going on steady state behaviour, up to 80-120 m sliding distance according to applied loads, and friction behaviours of the tested samples are getting increase sharply up to 0.6-0.7 friction coefficient value and going on steady state. As shown from the figure that, all the tested sample behaviour were same. However, the friction coefficient period of 10 N applied load sample with sliding distance was much higher than that of the others. Friction tests of the hard materials, in the initial period, the friction coefficient is getting increase up to steady state in general, because of the running in of the surface roughness of the worn couples. It was shown that from the figure that the wear mode of the tested samples were changed about 80-120 m sliding distance sharply. It is possible that the worn asperities from the surface caused to scratch the worn track of the samples and changed the wear mode from polishing effect to abrasive. In addition, increase in load values doesn't have an effect on the friction coefficient value of testing loads and friction coefficient of the tested samples close up each other.

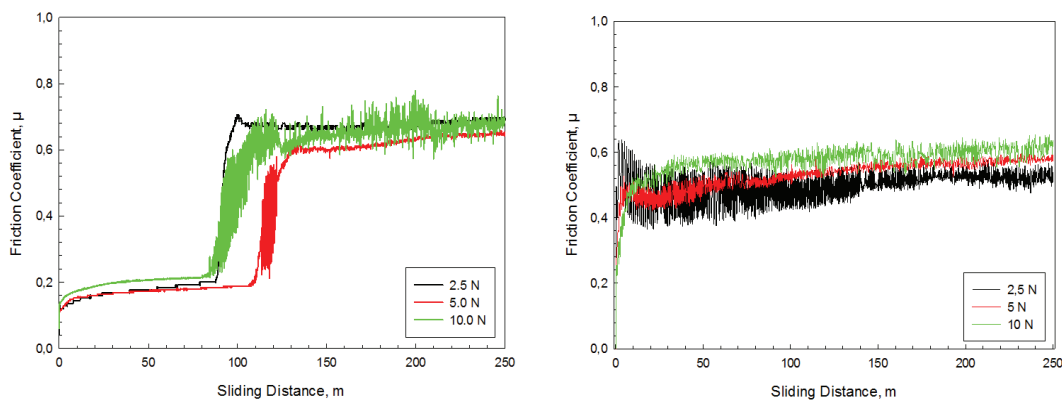


Figure 3 The friction coefficients of surface alloyed with Fe-W and Fe-W-B alloys on AISI 1020 steel under various loads

The wear rate of the samples was calculated from the cross-sectional area of the wear track measured by linear height profiles. The depth of the wear track was determined by averaging the lowest point in the center of the three line scans from profile-meter results. The reported depth of the wear track was quantified by averaging the lowest point in the center of the three line scans. The calculated worn areas for the three line scans were averaged and used as a surrogate measure of worn volume.

As shown from **Figure 5** that, increase in load value caused to increase of wear rate of the surface alloyed steel by Fe-W and Fe-W-B alloys, and the results showed that both of the

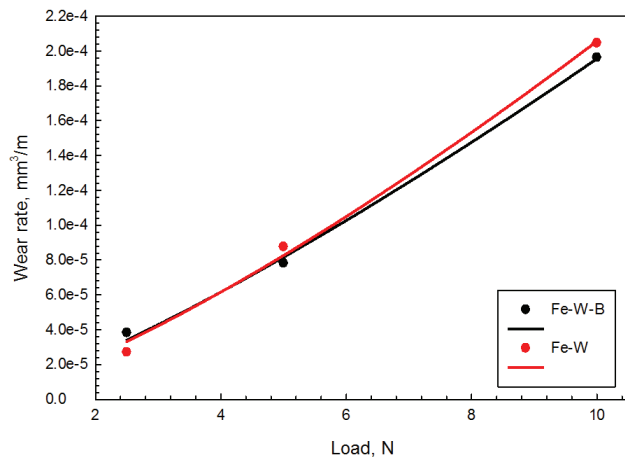


Figure 4 The wear rate of surface alloyed with Fe-W and Fe-W-B alloys of AISI 1020 steel

surface alloying treatment showed almost similar results. The wear rate of the surface alloyed layer with Fe-W alloys was slightly higher than that of the surface alloyed layer with Fe-W-B alloys. Wear rates on the surface alloyed layer of both alloys were changing linearly with increase in load values.

Figure 5 (a) and (b) present typical SEM micrographs for worn surfaces of the surface alloyed layers of both alloys against alumina. It is clear from those figures that wear behaviour of the surface alloyed layer with Fe-W alloy tested under the loads of 5 N showed that the worn track includes cracks networks and some spallation. In addition, these grey colour oxidative products took place during the wear tests. EDS analysis of the wear tracks showed that some oxygen peaks was seen together with Fe and W elements. As shown the worn surface SEM micrograph that the mod of the wear was micro abrasive, oxidative and fatigue wear. Whereas, wear mechanism of the Fe-W-B alloyed layers under the same conditions showed that the fingerprint structure of the eutectic morphology caused to the layered structure with pressure of the ball and bending effects. So, the alloyed layer presented to higher sustainability than the Fe-W based surface alloyed layer, because of the lamellar structure of the alloyed layer. SEM micrograph of the Fe-W-B hard faced layer showed that wear mode was oxidative and adhesive. In addition this, some fatigue cracks realized. However, it was not a crack network. It was individual cracks, which was different from the Fe-W surface alloyed layers worn surfaces.

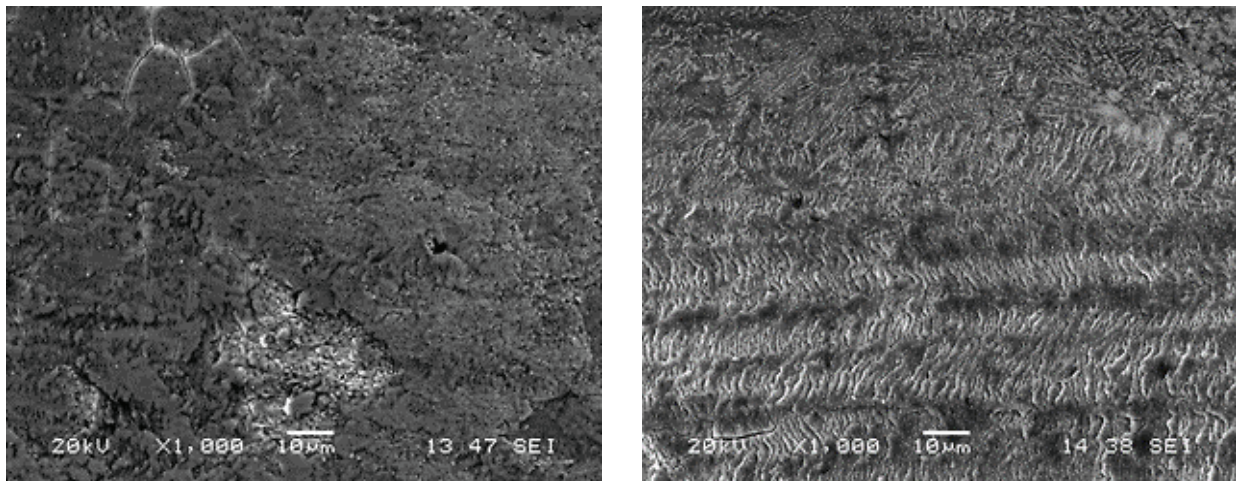


Figure 5 SEM micrographs of surface alloyed with (a) Fe-W and (b) Fe-W-B alloys on AISI 1020 steel against alumina ball under 5.0 load

4. CONCLUSIONS

Based on the results of the present study, it can be concluded that hardfacing, that performing with the Fe-W and Fe-W-B alloys on AISI 1020 steel substrate alters the microstructure of the hypereutectic alloy with Fe₇W₆, W-Fe solid solution and, FeWB, FeW₂B₂ and Fe₂W₂C phases, respectively. Boron addition to the Fe-W alloy changes the morphology of the microstructure, which is primarily responsible for wear resistance of the alloyed layers. In case of the Fe-W-B deposit, large primary borides and eutectic lamellar structure resist the deformation and increase the frictional forces resulting in high wear resistance. Further, oxide layers formed on the surface and their adherence to the surface also vary with the composition of the hardfacing alloy and this appears to influence the wear behavior of the coatings. Results also show that the oxidative, micro abrasive and fatigue wear was shown on the worn track of the surface alloyed layer of Fe-W alloy, while oxidative, adhesive and fatigue wear was determined on the worn surface of the alloyed layer of Fe-W-B alloy.

ACKNOWLEDGEMENTS

This work was financially supported by the Sakarya University, Department of Scientific Research Projects Unit No. 2016-01-08-009.

REFERENCES

- [1] LIU J., YANG S., XIA W., JIANG X., GUI C. Microstructure and wear resistance performance of Cu-Ni-Mn alloy based hardfacing coatings reinforced by WC particles. *Journal Alloys Compounds*, 2016, vol. 654, pp. 63-70.
- [2] YUAN L., HAN J., LIU J., JIANG Z. Mechanical properties and tribological behavior of aluminum matrix composites reinforced with in-situ AlB₂ particles. *Tribology International*, 2016, vol. 98, pp. 41-47.
- [3] LU-STEFFES O. J., SAKIDJA R., BERO J., PEREPEZKO J. H. Multicomponent coating for enhanced oxidation resistance of tungsten. *Surface and Coatings Technology*, 2012, vol. 207, pp. 614-619.
- [4] YAZICI S., DERIN B. Effects of process parameters on tungsten boride production from WO₃ by self-propagating high temperature synthesis, *Mater. Sci. Eng. B*, 2013, vol. 178, no. 1, pp. 89-93.
- [5] YANG K., YANG Q., BAO Y. Effect of carbonitride precipitates on the solid/liquid erosion behaviour of hardfacing alloy, *Appl. Surf. Sci.*, 2013, vol. 284, pp. 540-544.
- [6] YÜKSEL N., ŞAHİN S. Wear behavior-hardness-microstructure relation of Fe-Cr-C and Fe-Cr-C-B based hardfacing alloys, *Mater. Des.*, 2014, vol. 58, pp. 491-498.
- [7] FAN C., CHEN M.-C., CHANG C.-M., WU W. Microstructure change caused by (Cr,Fe)₂₃C₆ carbides in high chromium Fe-Cr-C hardfacing alloys, *Surf. Coat. Technol.*, 2006, vol. 201, no. 3-4, pp. 908-912.
- [8] KANNAN S., SENTHIL KUMARAN S., KUMARASWAMIDHAS L. A. An investigation on compression strength analysis of commercial aluminum tube to aluminum 2025 tube plate by using TIG welding process, *J. Alloys Compd.*, 2016, vol. 666, pp. 131-143.
- [9] SELÇUK B., IPEK R., KARAMIŞ M. B. A study on friction and wear behavior of carburized, carbonitrided and borided AISI 1020 and 5115 steels, *J. Mater. Process. Technol.*, 2003, vol. 141, no. 2, pp. 189-196.
- [10] V. RAGHAVAN, B-Fe-W (Boron-Iron-Tungsten), *J. Phase Equilibria*, 2003, vol. 24, no. 5, pp. 457-458.
- [11] LI Q., ZHOU D., ZHENG W., MA Y., CHEN C. Global Structural Optimization of Tungsten Borides, *Phys. Rev. Lett.*, 2013, vol. 110, no. 13, p. 136403.
- [12] BINDAL C., ÜÇİSİK A. H. Characterization of borides formed on impurity-controlled chromium-based low alloy steels, *Surf. Coat. Technol.*, 1999, vol. 122, no. 2-3, pp. 208-213.
- [13] JOHNSTON J. M., CATLEDGE S. A. Metal-boride phase formation on tungsten carbide (WC-Co) during microwave plasma chemical vapor deposition, *Appl. Surf. Sci.*, 2016, vol. 364, pp. 315-321.